Published by Avanti Publishers

International Journal of Petroleum Technology

ISSN (online): 2409-787X

Study on the Influence Law of Temperature Profile of Water Injection Well

Zhu Hanbin[1], Liu Wenqiang[1], Luo Hongwen[2,*], Li Haitao[2], Ma Hansong[2], Li Ying[2], Xiang Yuxing[2] and Zhang Qin[2]

[1]*CNPC Logging Co., Ltd, Xi'an 710077, China*

[2]*State Key Laboratory of Oil and Gas Reservoir Geology and Exploitation, Southwest Petroleum University, Chengdu 610500, China*

ARTICLE INFO

Article Type: Research Article

Academic Editor: Abarasi Hart

Keywords:
DTS
Orthogonal test
Water injection well
Temperature profile prediction model
The influence law of temperature profile

Timeline:
Received: March 01, 2023
Accepted: April 10, 2023
Published: May 10, 2023

Citation: Hanbin Z, Wenqiang L, Hongwen L, Haitao L, Hansong M, Ying L, Yuxing X, Qin Z. Study on the influence law of temperature profile of water injection well. Int J Petrol Technol. 2023; 10: 1-13.

DOI: https://doi.org/10.15377/2409-787X.2023.10.1

ABSTRACT

Due to the lack of knowledge on the influence law of the temperature profile of layered water injection wells, it is still highly challenging to quantitatively diagnose the water injection profile of layered water injection wells using distributed optical fiber temperature sensing (DTS). In this paper, a temperature profile prediction model for layered water injection wells has been developed by considering the micro-thermal effect and non-isothermal reservoir seepage. The influence of various single-factor changes on the temperature profile of layered water injection wells is simulated and analyzed. Orthogonal experiment analysis results demonstrate that the sensitivity of different factors on wellbore temperature from strong to weak is the injection temperature of the water, injection time, water injection rate, wellbore diameter, formation thermal conductivity, wellbore trajectory, and the permeability of injection formations (T_{inj}>t>Q_{inj}>D>K_t>θ>k). The injection temperature of water, injection time, and water injection rate are the dominant factors affecting the temperature profile of water injection wells. The results of this paper provide a theoretical foundation for the accurate evaluation of the water injection profile and water injection scheme optimization for the layered water injection wells.

*Corresponding Author
Email: rojielhw@163.com
Tel: +(86) 13512368947

1. Introduction

Water injection technology is crucial for enhancing crude oil recovery and the advantages of oilfield development since it is one of the most efficient oilfield stimulation strategies [1]. Unfortunately, technical issues such as unknown water injection profiles resulted in difficulties in water injection effect evaluation frequently arise [2]. It's extremely difficult to measure the water injection well directly using conventional tools. To quantitatively assess the water injection profile of water injection wells, it is vital to design a low-cost and high-accuracy monitoring system for the entire well section.

With the benefits of fully distributed sensing, high sensitivity, and high positioning precision [3-5], the distributed optical fiber temperature sensing (DTS) technology provides outstanding advantages in real-time monitoring of the temperature profile of the entire well section [6, 7]. To diagnose subterranean water outlet locations [8, 9], monitor casing leakage [10, 11], evaluate production profiles [12, 13], and other issues, DTS technology is increasingly employed in oilfields. Yet, comprehension of the wellbore temperature profile's changing law is required to quantitatively evaluate the downhole production and injection profile by DTS monitoring [14]. Thus, researchers around the world have carried out many studies on simulating the downhole temperature field.

By assuming single-phase flow in the tubing or casing, omitting the vertical wellbore friction pressure drop, and using temperature as a function of depth and production time, Ramey *et al*. [15] developed the first wellbore temperature model. Based on the heat conduction mechanism between the formation and the water injection wells, Feng Enmin *et al*. [16] proposed a mathematical model to simulate the temperature field of water injection wells, however, the model did not consider the properties of the layered formation. Based on the characteristics of water injection wells, Gao Peng [17] and Xiao Zhanshan [18] developed a temperature prediction model considering the coupling of the wellbore and formation models. Then, the effects of water injection volume, temperature, and other factors on the temperature profile are simulated and analyzed.

However, micro-heat effects like the Joule-Thompson effect are not included in their model, which makes it challenging to accurately simulate the small changes in the wellbore temperature profile. Based on Ramey's temperature model, a two-phase flow temperature prediction model is developed by Sagar *et al*. [19] considering the Joule-Thomson effect and kinetic energy impact. Nevertheless, this model is only applicable to incline deviated wells. Then, a temperature prediction model of the horizontal well was proposed by Yoshiok *et al*. [20] considering the partial microthermal effect. Based on the temperature profile simulation, the positions of the gas/water inflow were identified according to the DTS measurement for a field horizontal well [21]. A new temperature prediction model considering the multiphase flow of the horizontal well was developed by Zhu Shiyan [22] The temperature prediction model served as a forward model to quantitatively interpret and analyze the production profile of the horizontal well by inversion of DTS data. Furtherly, considering the temperature characteristics of the hydraulic fractures, more temperature models were developed to simulate the temperature profile of fractured horizontal wells [23, 24]. The influence of water production distribution on the wellbore temperature profile was examined as well.

Although many studies of the temperature behavior of vertical/horizontal wells in oil/gas reservoirs have been performed, the existing temperature profile prediction models are mostly applicable to horizontal wells. A conventional temperature prediction model can not be applied to describe the characteristics of water injection wells. Additionally, there is research on discussing the influence law of temperature profiles of water injection wells.

Therefore, this paper proposes to develop a new temperature prediction model for water injection wells based on mass and energy conservation, which is used to simulate and analyze the distribution characteristics and influence rules of the temperature profile of water injection wells. Subsequently, based on the theoretical simulation, the influence of several single factors on the temperature profile of the water injection well is analyzed. Through orthogonal test analysis, the sensitivity of the temperature profile on different affecting factors is evaluated to confirm the key factor affecting the temperature profile of the water injection well. It provides

theoretical model basics for the appropriate evaluation of the water injection effect and the quantitative interpretation of the water injection profile based on DTS monitoring.

2. Temperature Prediction Model of Water Injection Well

2.1. Formation Temperature Model

The heat transfer area in the formation of a water injection well includes the injection area and surrounding rock. The heat transfer mode includes heat conduction and heat convection. The heat transfer between formation and wellbore is shown in Fig. (**1**).

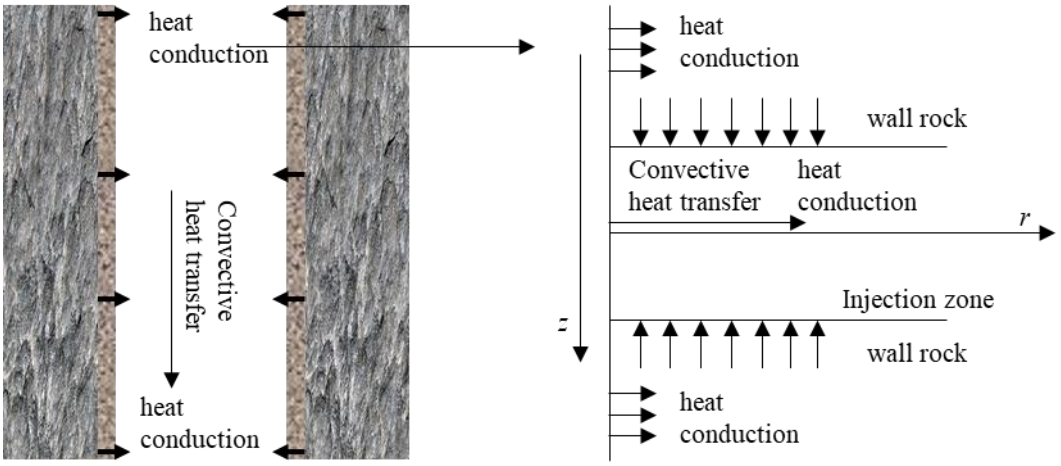

Figure 1: Heat transfer diagram of water injection well.

2.1.1. Formation Seepage Model

The continuity equation of multiphase flow is determined by the principle of mass conservation [25]:

$$-\nabla \cdot (\rho_i u_i) = \frac{\partial}{\partial t}(\phi \rho_i S_i) \tag{1}$$

Darcy's law of multiphase fluid flow and the addition of relative permeability allows for the formulation of the following non-isothermal flow model for water injection wells [22]:

$$\frac{1}{\rho_o}\nabla \cdot \left[\frac{\rho_o k k_{\mathrm{ro}}}{\mu_o}(\nabla p_o - \rho_o g \nabla D)\right] + \frac{1}{\rho_w}\nabla \cdot \left[\frac{\rho_w k k_{\mathrm{rw}}}{\mu_w}(\nabla p_w - \rho_w g \nabla D)\right] = \phi S_o c_o \frac{\partial p_o}{\partial t} + \phi S_w c_w \frac{\partial p_w}{\partial t} \tag{2}$$

Where, ρ_o andρ_w are the density of oil and water respectively, kg/m^3; ϕ is porosity; k is permeability of formation, D; k_{ro}、 k_{rw} represents respectively the relative permeability of oil and water; μ_0、 μ_w represents respectively the viscosity of oil and water, mPa·s; p_o、 p_w represents respectively pressure of oil and water, MPa; g is the acceleration of gravity, 9.8m/s^2; D is the vertical depth, and downward is positive, m.

Initial conditions:

$$\begin{cases} p(x,y,z,t)\big|_{t=0} = p_i \\ \mathrm{S}_w(x,y,z,t)\big|_{t=0} = \mathrm{S}_{wi} \end{cases} \tag{3}$$

Boundary conditions:

$$\begin{cases} p\big|_G = f_p(x,y,z,t) \\ \dfrac{\partial p}{\partial n}\Big|_G = f_q(x,y,z,t) \\ r\dfrac{\partial p}{\partial r}\Big|_{r=r_w} = \dfrac{q\mu}{2\pi kh} \\ p\big|_{r=r_w} = p_{wf}(x,y,z,t) \end{cases} \tag{4}$$

Where, p_i is the initial formation pressure, MPa; p_{wf} is the bottom hole pressure, MPa; S_{wi} is the original water saturation; The subscript G represents the boundary; n is the outer normal direction of boundary G; r_w is the borehole radius, m.

2.1.2. Formation Temperature Model

2.1.2.1. Injection Layers

According to the energy conservation in porous media, the temperature field model of the injection layer may be built for oil-water two-phase flow:

$$-\left[\sum_i (\phi\rho_i S_i C_{pi}) + (1-\phi)\rho_r C_{pr}\right]\frac{\partial T}{\partial t} + \sum\left(\phi S_i \beta_i \frac{\partial p_i}{\partial t}\right)T = \sum \rho_i u_i C_{pi}\nabla T - \sum \beta_i T(u_i \nabla p_i) + \sum \rho_i g u_i \cdot \nabla D \tag{5}$$

Where, C_{pr} is specific heat capacity, J/(kg·℃); β is the isobaric thermal expansion coefficient, 1/℃; λ is the thermal conductivity, W/(m·℃); The lower corner r is rock.

2.1.2.2. Non-Injection Layers

Because there is no fluid flow in the non-injection layer, the heat transfer process can be referred to as heat conduction. Equation (6) can be used to determine the temperature field model of the non-injection layer if the seepage velocity is 0:

$$(\rho c)^* \frac{\partial T}{\partial t} = \nabla(\lambda \nabla T) \tag{6}$$

Where $(\rho c)^*$ is the equivalent heat capacity of porous media:

$$(\rho c)^* = (1-\varphi)(\rho_s c_s) + \varphi(\rho_l c_l) \tag{7}$$

Where, c_s is the solid relative heat capacity, J/(kg·℃); c_l is the liquid relative heat capacity, J/(kg·℃).

2.2. Wellbore Temperature Model

Fig. (**1**) illustrates how the injected water travels through the wellbore and into the formation, where it is heated by convection and transferred to the reservoir. The steady-state wellbore temperature equation of multiphase flow is established as follows based on the conservation of mass and energy:

$$\frac{dT}{dx} = \frac{\left(\rho v C_p K_{JT}\right)_T}{\left(\rho v C_p\right)_T}\frac{dp}{dx} + \frac{2U_{T,I}}{R\left(\rho v C_p\right)_T}(T_I - T) - \frac{(\rho v)_T}{\left(\rho v C_p\right)_T} g\sin\theta \tag{8}$$

Including:

$$K_{JT} = \frac{\beta T - 1}{\rho C_p} \tag{9}$$

$$(\rho v)_T = \sum_i \rho_i v_i h_i \tag{10}$$

$$\left(\rho v C_p\right)_T = \sum_i \rho_i v_i h_i C_{pi} \tag{11}$$

$$\left(\rho v C_p\right)_{T,I} = \sum_i \rho_{i,1} v_{i,1} h_{i,1} C_{pi} \tag{12}$$

$$\left(\rho v C_p K_{JT}\right)_T = \sum_i \rho_i v_i h_i C_{pi} K_{JT,i} \tag{13}$$

$$U_{T,I} = \gamma\left(\rho v C_p\right)_{T,I} + (1-\gamma)U \tag{14}$$

Where, K_{JT} is Joule-Thomson coefficient, ℃/MPa; $U_{T,I}$ is the comprehensive heat transfer coefficient of the shaft, W/(m^2·℃); T_I is the temperature at the sand surface of the borehole, ℃.

In this work, the developed reservoir models and wellbore models are coupled, and the coupled model is solved numerically to obtain the wellbore temperature profile. Fig. (**2**) shows a schematic of the solution procedure for the coupled temperature model.

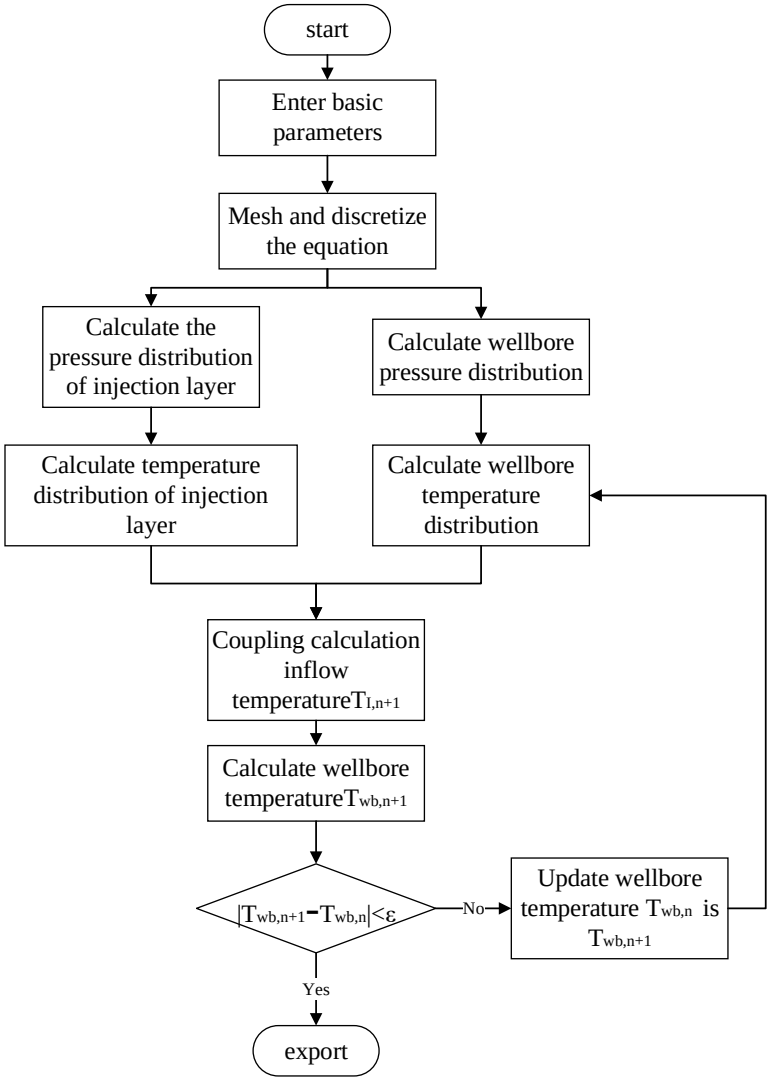

Figure 2: Calculation flow chart of wellbore temperature profile of water injection well.

3. Influence Law and Sensitive Parameters Analysis of Temperature Profile for Water Injection Well

To study the impact of different factors on the temperature profile of water injection wells and confirm the primary controlling factors, the temperature prediction model developed in this paper is used to simulate and analyze the temperature profile of layered water injection wells. The basic parameters of the simulated water injection well and formation layers are listed in Table **1** and Table **2**.

Table 1: Basic parameters of the simulated water injection well.

Parameter	Numerical Value	Parameter	Numerical Value
Injection pressure， Mpa	12	Specific heat capacity of oil pipe， J/(kg·℃)	487
Water injection rate，m^3/h	25	Specific heat capacity of casing， J/(kg·℃)	487
Specific heat capacity of formation rock，J/(m^3·K)	845	Reservoir thickness，m	20
Thermal conductivity of formation rock，W/(m·℃)	4.46	Geothermal gradient，℃/m	0.03
Specific heat capacity of cement ring，J/(kg·℃)	210	Ground temperature，℃	20
Injection water temperature，℃	18	Formation pressure， MPa	15
Formation porosity	0.12	Water saturation	0.8
Inner diameter of cement sheath，m	0.1778	Thermal conductivity of water phase，W/m·℃	0.673
Outer diameter of cement sheath，m	0.2400	Thermal conductivity of technical casing，W/(m·℃)	53
Inside diameter of oil pipe，m	0.114	Thermal conductivity of oil pipe，W/(m·℃)	53
Outer diameter of oil pipe，m	0.120	Water phase viscosity，cp	0.34
Inner diameter of technical casing，m	0.1594	Surface casing diameter，m	0.34
Outer diameter of technical casing，m	0.1778	Specific heat capacity of oil pipe，J/(kg·℃)	487

Table 2: Basic parameters of the injection layers.

Order Number	Top Depth，m	Bottom Depth，m	Permeability，mD	Porosity	Average Pressure，MPa
Injection layer 1	500	600	2	0.12	9
Injection layer 2	700	750	1.5	0.11	9.5
Injection layer 3	800	900	2.5	0.13	10

3.1. Analysis of Single Factor Influence Law of Temperature Profile for Water Injection Well

By simulating the temperature dynamics under various single factors, this section examines the effects of seven different single factors on the temperature profile of the aforementioned abstract water injection wells. When exploring the impact of various single factors on the temperature profile, keep the other factors unchanged.

3.1.1. Influence of Water Injection Rate

Fig. (**3**) depicts the wellbore temperature profile for various injection rates. As seen in Fig. (**3a**), the wellbore temperature profile decreases as the injection rate increases. Because the higher the injection rate, the shorter the heat exchange time between wellbore fluid and formation in unit volume, the greater the total amount of low-

temperature fluid in the wellbore, the lower the heating capacity of the reservoir to the injected water, and the lower the wellbore temperature profile. The wellbore flow profile is shown in Fig. (**3b**). It demonstrates that the wellbore flow profile of the injection well has a "ladder" form, with each "ladder" location denoting a different injection layer. The reservoir permeability, in general, regulates how much water is absorbed by each layer.

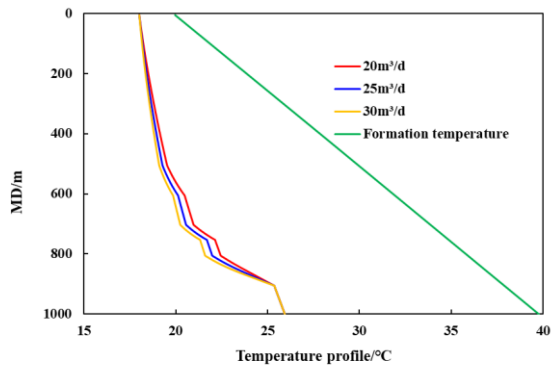

(a) Wellbore temperature profile

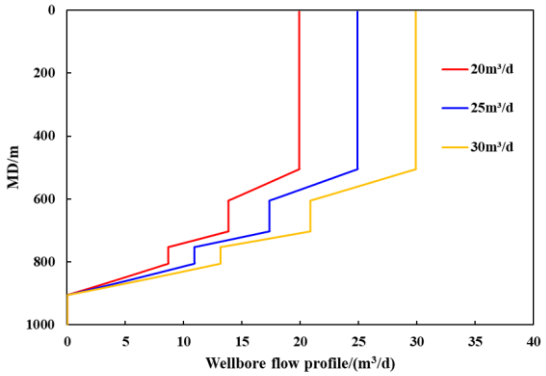

(b) Wellbore flow profile

Figure 3: Effect of water injection on temperature profile.

3.1.2. Influence of Water Injection Temperature

Fig. (**4**), which depicts the wellbore temperature profile under various water injection temperatures, shows that the overall wellbore temperature profile increases with increasing water injection temperature. No matter how the temperature of the injected water changes, the wellbore temperature profile always stays near the ground temperature profile because the fluid in the wellbore is mostly affected by the ground temperature when flowing in the wellbore. The more the temperature profile differs from the ground temperature, the faster the temperature profile changes due to the formation's increased heat transfer efficiency. The water injection profile is mostly governed by the reservoir permeability distribution, as shown in Fig. (**4b**). However, when the water injection temperature increase, the water absorption of injection formation layers close to the wellhead increases relatively, and the water absorption of injection formation layers close to bottom decrease slightly.

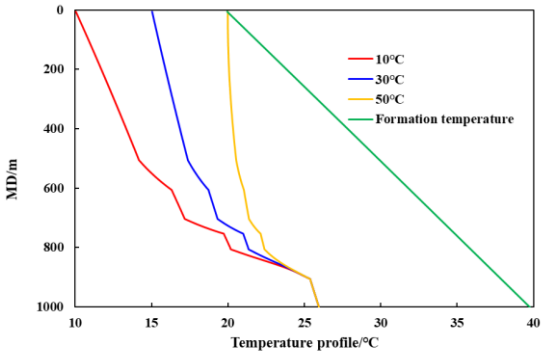

(a) Wellbore temperature profile

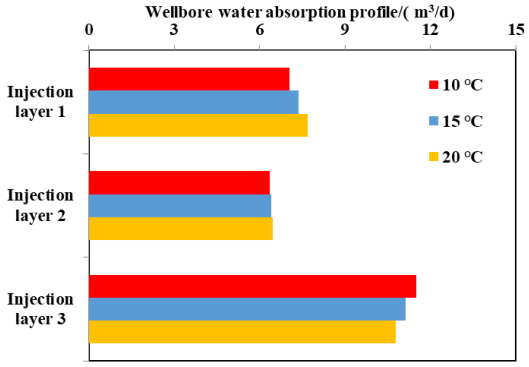

(b) Wellbore water absorption profile

Figure 4: Effect of injected water temperature on temperature profile.

3.1.3. Influence of Formation Thermal Conductivity

Fig. (**5a**) illustrates the wellbore temperature profile under different formation thermal conductivity. It demonstrates that the greater the formation thermal conductivity is, the higher the overall wellbore temperature profile of the water injection well is when the water injection rate and injection temperature keep constant. Because, heat transfers of the rock are more efficient when the thermal conductivity of the formation rises

throughout the water injection process, and heat conduction per unit time also rises. Fig. (**5b**) again demonstrates that the formation of thermal conductivity has a very slight effect on the water injection profile.

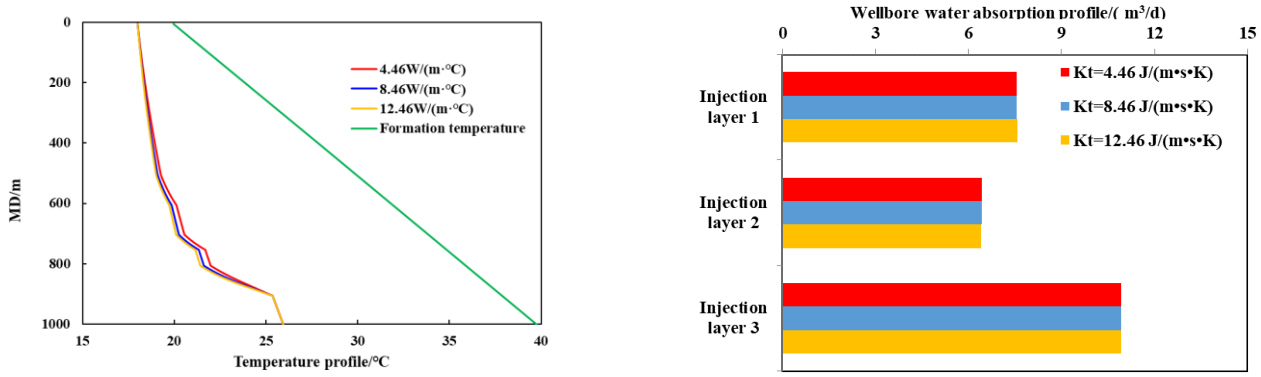

(a) Wellbore temperature profile **(b) Wellbore water absorption profile**

Figure 5: Effect of formation thermal conductivity on wellbore temperature profile.

3.1.4. Influence of Wellbore Diameter

Fig. (**6a**) shows the temperature profils of water injection well under various well diameters. It is clear from Fig. (**6a**) that when the wellbore diameter increases, the temperature profile of water injection wells decreases. Because, with a given water injection rate, larger wellbore diameter results in a decreased wellbore fluid flow velocity. Then, wellbore friction resistance is decreased, and the heat generated by the friction effect is diminished. Fig. (**6b**) demonstrates that the water injection profile is still positively connected with the reservoir permeability distribution while the wellbore diameter has minimal effect on the profile.

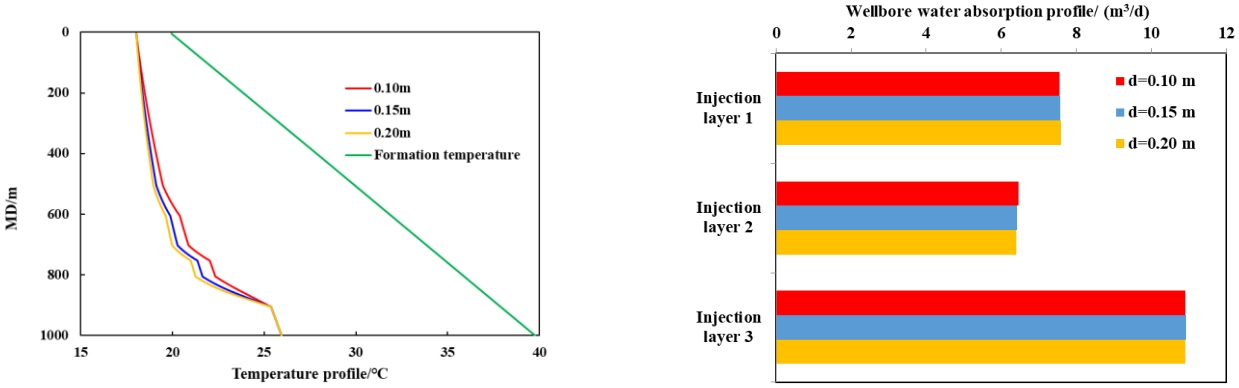

(a) Wellbore temperature profile **(b) Wellbore water absorption profile**

Figure 6: Effect of wellbore diameter on wellbore temperature profile.

3.1.5. Influence of Injection Time

Fig. (**7**) shows the temperature profiles of water injection well under different injection times (1, 3, and 5 hours). As shown in Fig. (**7a**), the wellbore temperature profile generally decreases with increasing injection time. Moreover, the change rate of the wellbore temperature profile considerably reduces as injection time increases. This is mostly due to the significant temperature differences at the beginning of injection between the wellbore and the formation. The heat exchange eventually becomes adequate with an increase in injection time, resulting in a reduction in the change of the wellbore temperature profile at the same time interval. Although the effect of water injection time on the water injection profile is typically negligible, Fig. (**7b**) shows that the water absorption

of injection formation layers close to the bottom increase relatively, and the water absorption of injection formation layers close to the wellhead decrease slightly during the water injection process.

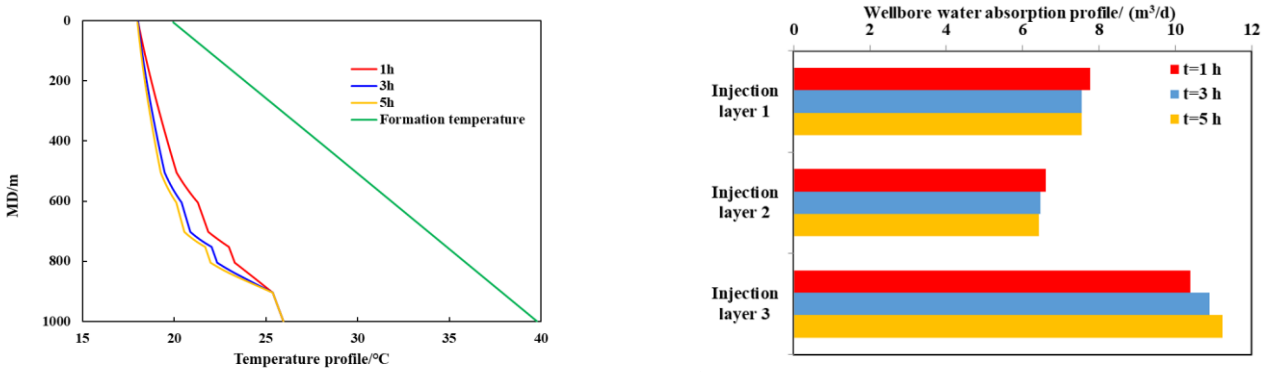

(a) Wellbore temperature profile **(b) Wellbore water absorption profile**

Figure 7: Effect of water injection time on wellbore temperature profile.

3.1.6. Influence of Well Trajectory

The wellbore temperature profile under various wellbore trajectories is depicted in Fig. (**8**). It shows that the wellbore temperature profile decreases with the increase of the wellbore dip angle (θ). Because the wellbore vertical depth and the geothermal profile generally decrease with an increase of θ. The water injection profile is still governed by the formation permeability distribution, and the dip angle has little impact on the water injection profile (Fig. **8b**).

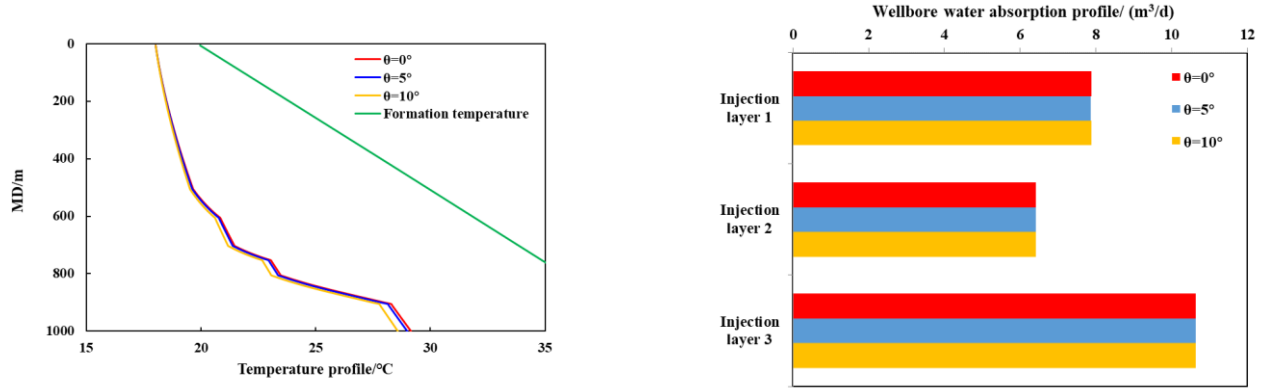

(a) Wellbore temperature profile **(b) Wellbore water absorption profile**

Figure 8: Effect of well path on wellbore temperature profile.

3.1.7. Influence of the Permeability of the Formation Layers

The wellbore temperature profile under different permeability distribution (the relative permeability of each injection layer remains constant) of the injection formation are shown in Fig. (**9**). It demonstrates that the wellbore temperature profile is only marginally affected by changes in the average permeability of the injection layers. The wellbore temperature profile marginally rises when the average permeability of the injection formation increases. When the permeability distribution of the formation layers changes (the permeability of each injection layer is different, showing in Table **3**), the wellbore temperature profile of the injection well will significantly change even if under the same injection rate (25 m^3/d) and average injection layer permeability (2mD). According to Fig. (**9c**), the distribution trend of the wellbore temperature profile corresponds to the water injection profile. Comparatively speaking, permeability distribution has a significant impact on the water injection profile that in turn affects the distribution trend of the temperature profile.

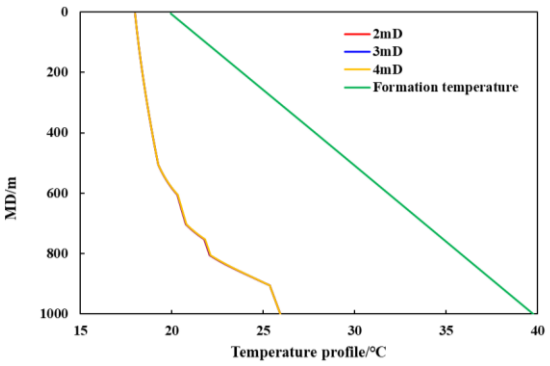

(a) Influence of average permeability on the temperature profile

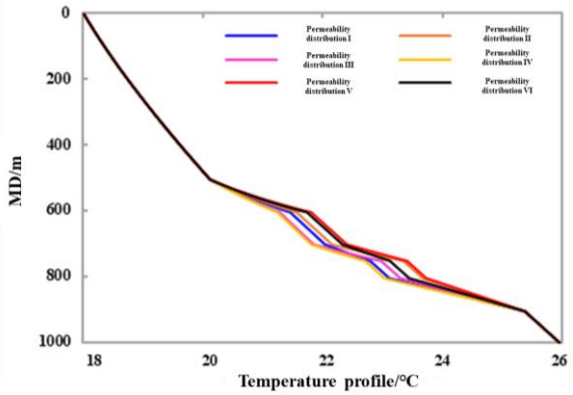

(b) Influence of permeability distribution on the temperature profile

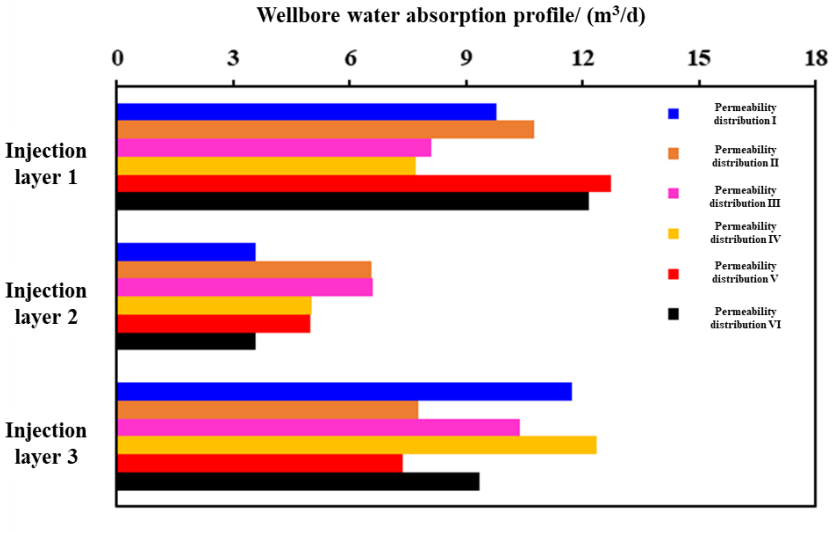

(c) Wellbore water absorption profile

Figure 9: Effect of water injection layer permeability on wellbore temperature profile.

Table 3: Permeability distribution of water injection layers.

Injection Layer Permeability（mD）	Injection Layer 1	Injection Layer 2	Injection Layer 3
Permeability distribution I	2	1.5	2.5
Permeability distribution II	2	2.5	1.5
Permeability distribution III	1.5	2.5	2
Permeability distribution IV	1.5	2	2.5
Permeability distribution V	2.5	2	1.5
Permeability distribution VI	2.5	1.5	2

3.2. Sensitive Parameters Evaluation of the Temperature Profile for Water Injection Well

In this study, sensitivity analysis of different factors affecting the temperature profile of the water injection well is conducted using the orthogonal test analysis approach. The basic parameters needed for the simulation calculations are listed in Tables **1** and **2**. The water injection rate (Q_{inj}), water injection temperature (T_{inj}), formation thermal conductivity (K_t), wellbore diameter (D), water injection time (t), average permeability of injection layer (k),

and well trajectory (θ) are selected as the seven influencing factors based on the setting of analysis factors. In the orthogonal test design, there are 7 factors, and three levels of each factor are included (Table **4**).

Table 4: Analysis factors and level design of orthogonal test.

Factor Name	Q_{inj}, m^3/d	T_{inj}, ℃	K_t, W/(m·℃)	t, h	k,D	D, m	θ, °
Level 1	20	10	4.46	1	2	0.10	0
Level 2	25	15	8.46	3	3	0.15	5
Level 3	30	20	12.46	5	4	0.20	10

The standard orthogonal table (Table **5**) of L_{18} (3^7) was chosen for the orthogonal test analysis by the design of the orthogonal test system. The assessment measure used to quantify the overall change in the temperature profile of the water injection well is the average temperature difference between the geothermal profile and the wellbore temperature profile. The results of the orthogonal test are listed in Table **5**. It demonstrates that the

Table 5: Analysis results of orthogonal test.

Experiment No.	Q_{inj}	T_{inj}	K_t	D	t	k	θ	Average Temperature Difference, ℃
Experiment 1	1	1	1	1	1	1	1	33.444
Experiment 2	1	2	2	2	2	2	2	40.158
Experiment 3	1	3	3	3	3	3	3	36.759
Experiment 4	2	1	1	2	2	3	3	45.373
Experiment 5	2	2	2	3	3	1	1	44.513
Experiment 6	2	3	3	1	1	2	2	34.432
Experiment 7	3	1	2	1	3	2	3	47.784
Experiment 8	3	2	3	2	1	3	1	40.414
Experiment 9	3	3	1	3	2	1	2	37.146
Experiment 10	1	1	3	3	2	2	1	47.903
Experiment 11	1	2	1	1	3	3	2	37.463
Experiment 12	1	3	2	2	1	1	3	34.665
Experiment 13	2	1	2	3	1	3	2	45.535
Experiment 14	2	2	3	1	2	1	3	40.408
Experiment 15	2	3	1	2	3	2	1	36.329
Experiment 16	3	1	3	2	3	1	2	52.325
Experiment 17	3	2	1	3	1	2	3	40.851
Experiment 18	3	3	2	1	2	3	1	35.967
mean value 1	38.399	45.394	38.434	38.250	38.224	39.762	38.504	
mean value 2	41.098	40.634	41.437	41.544	41.159	41.177	41.243	
mean value 3	42.414	40.311	42.040	42.118	42.529	40.973	40.252	
Range(R)	4.015	5.083	3.606	3.868	4.305	1.415	2.739	
sort	third	first	fifth	fourth	second	seventh	sixth	
Order of influence degree:	$T_{inj}>t>Q_{inj}>D>K_t>\theta>k$							

sensitivity of different factors on wellbore temperature from strong to weak is the injection temperature of the water, injection time, water injection rate, wellbore diameter, formation thermal conductivity, wellbore trajectory, and the permeability of injection formations ($T_{inj}>t>Q_{inj}>D>K_t>\theta>k$). The injection temperature of water, injection time, and water injection rate are the dominant factors affecting the temperature profile of water injection wells.

The temperature prediction model proposed in this work can be used as the forward model. Combining with artificial intelligence techniques such SA algorithm [26, 27], and the MCMC algorithm [28] *et al*., an inversion model can be developed to interpret the DTS data of water injection well. It can realize the quantitative interpretation of the water injection profile from downhole temperature measurements. Then, technical issues in water injection effect evaluation can be addressed.

4. Conclusion

A temperature prediction model was proposed to simulate the temperature profile of the water injection well. Based on the temperature profile simulation, the influence law and sensitive parameters analysis of the temperature profile for the water injection well has been performed, the main conclusions can be drawn as follows:

1) The temperature simulation results demonstrated the capability of the developed model to predict the temperature behavior of a water injection well with layered formations.

2) For water injection well, the wellbore temperature profile decreases with the injection rate increase and increases with the water injection temperature increase. The more significantly the temperature profile differs from the geothermal temperature, the faster the temperature profile changes due to the formation's increased heat transfer efficiency. When the water injection temperature increase, the water absorption of injection formation layers close to the wellhead increases relatively, and formation layers close to the bottom decrease slightly. Greater formation thermal conductivity would result in a higher wellbore temperature profile. when the wellbore diameter increases, the temperature profile of water injection wells decreases. The wellbore temperature profile generally decreases with the increasing injection time. The wellbore temperature profile generally decreases with the increasing injection time and the wellbore temperature profile decreases with the increase of the wellbore dip angle (θ). The wellbore temperature profile marginally rises when the average permeability of the injection formation increases and the distribution trend of the wellbore temperature profile corresponds to the water injection profile.

3) The results of orthogonal test analysis demonstrate that the sensitivity of different factors on wellbore temperature from strong to weak is the injection temperature of the water, injection time, water injection rate, wellbore diameter, formation thermal conductivity, wellbore trajectory, and the permeability of injection formations ($T_{inj}>t>Q_{inj}>D>K_t>\theta>k$). The injection temperature of water, injection time, and water injection rate are the dominant factors affecting the temperature profile of water injection wells.

Acknowledgements

This study was funded by China Postdoctoral Science Foundation (Grant No. 2021M702721), Natural Science Foundation of Sichuan Province (Grant No. 2022NSFSC0993), SINO-GERMAN MOBILITY PROGRAMME (M0469), Natural Science Foundation of China (42272176), Scientific Research and Technology Development Program of China National Petroleum Corporation (2021DJ3803).

References

[1] Liu H, Pei X, Luo K, Sun F, Zheng L, Yang Q. Status quo and development trend of layered water injection technology for oil and gas field development in China. Pet Explor Dev 2013; 40: 785-90.

[2] Sui YY, Li ZP, Wang JQ, Ye YZ, Li YL. Prediction of water injection profile using implicit nonlinear method. Zhongguo Shiyou Daxue Xuebao (Ziran Kexue Ban)/Journal of China University of Petroleum (Natural Science). 2010; 34: 95-8. https://doi.org/10.3969/j.issn.1673-5005.2010.06.018

[3] Li Xiaorong, Liu X, Zhang Y, Fang G, Xindong W, Yongcun F. Application and progress of oil and gas well engineering monitoring technology based on distributed optical fiber acoustic sensor. Pet Drill Prod Proc. 2022; 44: 309-20.

[4] Kurashima T, Horiguchi T, Tateda M. Distributed-temperature sensing using stimulated Brillouin scattering in optical silica fibers. Opt Lett. 1990; 15: 1038-40. https://doi.org/10.1364/OL.15.001038

[5] Culverhouse D, Farahi F, Pannell CN, Jackson DA. Potential of stimulated Brillouin scattering as sensing mechanism for distributed temperature sensors. Electron Lett. 1989; 25: 913-5. https://doi.org/10.1049/el:19890612

[6] Luo H, Li H, Jiang B. A new interpretation method for production profile of fractured horizontal wells in low permeability gas reservoirs based on DTS data inversion. Nat Gas Geosci. 2019; 30: 1639-45.

[7] Luo H, Li H, An S. Analysis on influencing factors of temperature profile of fractured horizontal well in tight gas reservoir. Special Oil and Gas Reservoirs. 2021; 28: 150-7.

[8] Wheaton B, Haustveit K, Deeg W, Miskimins J, Barree R. A case study of completion effectiveness in the eagle ford shale using DAS/DTS observations and hydraulic fracture modeling, SPE Hydraulic Fracturing Technology Conference, The Woodlands, Texas, USA: SPE; 9-11 February 2016. https://doi.org/10.2118/179149-ms

[9] Achnivu OI, Zhu D, Furui K. Interpretation method of downhole temperature and pressure data for detecting water entry in inclined gas wells. SPE Annual Technical Conference and Exhibition, Denver, Colorado, USA: SPE; 21-24 September 2008. https://doi.org/10.2118/115753-MS

[10] Molenaar MM, Fidan E, Hill DJ. Real-time downhole monitoring of hydraulic fracturing treatments using Fibre Optic Distributed Temperature and acoustic sensing. SPE/EAGE European Unconventional Resources Conference and Exhibition, Vienna, Austria: SPE; 20-22 March 2012. https://doi.org/10.2118/152981-MS

[11] Ugueto GA, Huckabee PT, Molenaar MM. Challenging assumptions about fracture stimulation placement effectiveness using fiber optic distributed sensing diagnostics: diversion, stage isolation and overflushing. SPE Hydraulic Fracturing Technology Conference, The Woodlands, Texas, USA: SPE; 3-5 February 2015. https://doi.org/10.2118/SPE-173348-MS

[12] Zhang S, Zhu D. Inversion of downhole temperature measurements in multistage fracture stimulation in horizontal wells. SPE Annual Technical Conference and Exhibition, San Antonio, Texas, USA: SPE; 9-11 October 2017. https://doi.org/10.2118/187322-MS

[13] Li H, Luo H, Xiang Y, Li Y, Jiang B, Cui X, *et al*. DTS based artificial fracture identification and production profile interpretation method for shale gas horizontal wells. Natural Gas Industry. 2021; 8: 494-504. https://doi.org/10.1016/j.ngib.2021.05.001

[14] Hansong M, Luo H, Haitao L, Yuxing X, Qin Z, Ying L. Study on the influence law of temperature profile of vertical wells in gas reservoirs. Int J Pet Technol. 2022; 9: 54-66. https://doi.org/10.15377/2409-787X.2022.09.7

[15] Ramey HJ. Wellbore heat transmission. J Pet Technol. 1962; 14: 427-35. https://doi.org/10.2118/96-PA

[16] Feng E, Yan G, Hu Z. Numerical simulation and optimization of temperature field in formation zone of water injection well. J Pet. 1996: 96-102.

[17] Gao P. Numerical calculation of well temperature logging. Jilin University; 2007.

[18] Xiao Z. Numerical simulation of downhole temperature field of water injection well. Daqing Petroleum Institute; 2002.

[19] Sagar R, Doty DR, Schmldt Z. Predicting temperature profiles in a flowing well. SPE Prod Eng. 1991; 6: 441-8. https://doi.org/10.2118/19702-PA

[20] Yoshioka K, Zhu D, Hill AD, Dawkrajai P, Lake LW. Prediction of temperature changes caused by water or gas entry into a horizontal well. SPE Prod Oper. 2007; 22: 425-33. https://doi.org/10.2118/100209-PA

[21] Yoshioka K, Zhu D, Hill AD. A new inversion method to interpret flow profiles from distributed temperature and pressure measurements in horizontal wells. SPE Prod Oper. 2009; 24: 510-21. https://doi.org/10.2118/109749-PA

[22] Zhu S. Theoretical research on horizontal well production profile interpretation based on distributed optical fiber temperature measurement. Southwest Petroleum University; 2016.

[23] Yoshida N. Modeling and interpretation of downhole temperature in a horizontal well with multiple fractures (Thesis). Texas A&M University; 2016. https://doi.org/10.2118/181812-MS

[24] Luo Hongwen, Li Haitao, Liu Huibin. Prediction of temperature profile of two-phase flow fracturing horizontal well in low permeability gas reservoir. Nat Gas Geosci. 2019; 30: 389-99.

[25] Zhai Y. Seepage mechanics. Petroleum Industry Press; 2016.

[26] Hongwen L, Haitao L, Yongsheng T, Ying L, Beibei J, Yu L, *et al*. A novel inversion approach for fracture parameters and inflow rates diagnosis in multistage fractured horizontal wells. J Pet Sci Eng. 2020; 184: 106585. https://doi.org/10.1016/j.petrol.2019.106585

[27] Hongwen L, Haitao L, Yu L, Ying L, Zhenhua G. Inversion of distributed temperature measurements to interpret the flow profile for a multistage fractured horizontal well in low-permeability gas reservoir. Appl Math Model. 2020; 77: 360-77. https://doi.org/10.1016/j.apm.2019.07.047

[28] Luo H, Li Y, Li H, Cui X, Chen Z. Simulated annealing algorithm-based inversion model to interpret flow Rate Profiles and fracture parameters for horizontal wells in unconventional gas reservoirs. SPE J. 2021; 26(04): 1679-99. https://doi.org/10.2118/205010-PA